Available online at www.sciencedirect.com
ScienceDirect
International Journal of Pharmaceutics 350 (2008) 361–368
INTERNATIONAL JOURNAL OF PHARMACEUTICS
www.elsevier.com/locate/ijpharm

Pharmaceutical Nanotechnology

Suspension of Fe_3O_4 nanoparticles stabilized by chitosan and *o*-carboxymethylchitosan

Aiping Zhu [a,*], Lanhua Yuan [a], Tianqing Liao [b]

[a] *College of Chemistry and Chemical Engineering, Yangzhou University, Yangzhou 225002, PR China*
[b] *Department of Chemical and Biomedical Engineering, Florida State University, Florida 32310, USA*

Received 25 May 2007; received in revised form 2 August 2007; accepted 2 September 2007
Available online 6 September 2007

Abstract

In this study, a well-dispersed suspension of superparamagnetic Fe_3O_4 nanoparticles was stabilized by chitosan (CS) and *o*-carboxymethylchitosan (OCMCS), respectively. The resulting magnetic Fe_3O_4 nanoparticles were characterized by dynamic light scattering (DLS), Fourier transform infrared spectroscopy (FTIR), X-ray diffraction (XRD), transmission electron microscope (TEM), zeta-potential measurement and vibrating sample magnetometry (VSM). TEM results demonstrated a spherical or ellipsoidal morphology with an average diameter of 14–20 nm. The adsorbed layer of CS and OCMCS on the magnetite surface was confirmed by FTIR. XRD illustrated that the resulting magnetic nanoparticles have a spinel structure and lastly VSM results showed the modified magnetic Fe_3O_4 nanoparticles were superparamagnetic. The adsorption mechanism of CS and OCMCS onto the surface of Fe_3O_4 nanoparticles is believed to be the electrostatic and coordination interactions, respectively. The mechanisms of both CS and OCMCS stabilizing the suspension of Fe_3O_4 nanoparticles were supposed electrostatic repulsion. These well-dispersed superparamagnetic Fe_3O_4 nanoparticles stabilized by the biocompatible CS or OCMCS dispersant should have potential applications in biotechnology fields.

Keywords: Superparamagnetic; Fe_3O_4; Nanoparticles; Well-dispersed; Chitosan; *o*-Carboxymethylchitosan

1. Introduction

The synthesis of uniformly sized magnetic nanoparticles has been intensively pursued because of their broad applications, including magnetic storage media, ferrofluids, magnetic resonance imaging, and magnetically guided drug delivery (Kim et al., 2001a,b; Reynolds et al., 2000; Lubbe et al., 1996; Chan et al., 1993; Jordan et al., 1999; Dyal et al., 2003; Neuberger et al., 2005; Morales et al., 2005). Various common protocols were developed to synthesize iron oxides, such as condensing divalent and trivalent iron salts in reactions with hydroxide bases (pH 9.5–10) (Mann and Hannington, 1988; Kim et al., 2001a,b; Zhang et al., 2002; Harris et al., 2003), and chemical oxidation in micelle media (Shen et al., 1999) or in polymer (Ma et al., 2005; Xie et al., 2004).

However, one of the main challenges facing almost all of these novel techniques is the ability to transport and deliver well-dispersed nanoparticles with the desired composition, structure, and uniformity as well as the prevention of aggregation (Chouly et al., 1996; Thode et al., 1997; Mahapatra et al., 2006). A crucial physical property of magnetic nanoparticles is their tendency to aggregate. Encounters between particles dispersed in liquid media occur frequently, and the stability of a suspension is determined by the interaction between the particles during these encounters. The principal cause of aggregation is the short-range forces—van der Waals attraction between the two particles. To counteract these attractive interactions and promote stability, equally short-range repulsive forces are required (Bonnemann et al., 2001). They are enforced either by electrostatic repulsion between the particles or by coating the particles with organic long-chain molecules (Chang et al., 2006; Zhi et al., 2006).

Magnetic nanoparticles can be dispersed in carrier fluid through specific interactions between the particle surfaces and selected low-molecular-weight surfactants or polymer. Various methods have been reported for the preparation of stable dispersions of iron oxide in organic solvents (organosols), including hexane and decane (Shafi et al., 2001; Fried et

* Corresponding author. Tel.: +86 514 7975568; fax: +86 514 7975524.
E-mail address: apzhu@yzu.edu.cn (A. Zhu).

0378-5173/$ – see front matter © 2007 Elsevier B.V. All rights reserved.
doi:10.1016/j.ijpharm.2007.09.004

al., 2001). However, for these organosols, the biological applications are greatly restricted because of their poor solubility in aqueous solutions. For biomedical applications, it is essential to develop nanoscale magnetite with a narrow size distribution and surface coating with biocompatibility materials, i.e., nonimmunogenic, nonantigenic, and protein-resistant (Xie et al., 2004; Chouly et al., 1996; Shieh et al., 2005).

Due to its biocompatibility and biodegradability, chitosan has been widely employed in tissue engineering and controlled drug/gene delivery (Kofuji et al., 2001; Thanou et al., 2001; Roy et al., 1999). Chitosan with net positive charge binds with recombinant DNA plasmids to form complex nanoparticles for delivering genes into cells (Mao et al., 2001; Artursson et al., 1994; Senel et al., 2000; Fang et al., 2001). The bio-adhesiveness of chitosan makes it an ideal candidate for mucosal drug delivery (Fang and Chan, 2003). For instance, the co-administration of chitosan with drugs has been shown to enhance the transcellular and paracellular transport of drugs across mucosal epithelium (Chan et al., 2001). Moreover, the overcoming of the cellular membrane barrier by chitosan-based gene carriers in the absence of receptor-mediated endocytosis has led to the hypothesis that chitosan directly interacts with cell membranes (Thanou et al., 2001). *o*-Carboxymethylchitosan (OCMCS) has a backbone structure similar to CS, but the *o*-hydroxyl group of each monomer is substituted by a carboxymethyl group through ether bond formation (Scheme 1). OCMCS has been shown to have amphiphilic, blood compatible and effective membrane penetrable properties (Zhu et al., 2005a,b). More strikingly, it can load hydrophobic anticancer drugs effectively (Zhu et al., 2006). Though lots of synthesized polymers (e.g., poly(vinyl alcohol) phosphate, polyethylene glycol, polyamides, polyglycidyl methacrylate, poly(acrylic acid)) were employed as a coating agent in the surface modification of iron oxide particles (Gas et al., 2006; Guo et al., 2007; Abu-Much et al., 2006; Wan et al., 2007; Xie et al., 2004), the natural polymeric and bioactive properties of chitosan and OCMCS lead our interest to explore the feasibility of synthesizing a well-dispersed aqueous dispersion of superparamagnetic Fe_3O_4 nanoparticles stabilized by CS or OCMCS, simply and effectively. The mechanisms of CS and OCMCS stabilizing the suspension of Fe_3O_4 nanoparticles were discussed in this study.

2. Experimental

2.1. Chemicals and materials

Ferric chloride hexahydrate ($FeCl_3{\cdot}6H_2O$, >99%), ferrous chloride tetrahydrate ($FeCl_2{\cdot}4H_2O$, >99%) and ammonium hydroxide (29.4%) were obtained from Shanghai Chemical Reagent (China). Chitosan was obtained from Lianyungang Biologicals Inc. (China). Its viscosity average molecular weight was 5.2×10^5 g/mol, and the degree of deacetylation was 90%. *o*-Carboxymethylchitosan, containing about 100 carboxyl groups and 75 amino groups per 100 anhydroglucosamine units of chitosan was prepared by methods we have previously reported (Zhu et al., 2005a,b). All the other chemicals were of reagent grade and used without further purification.

2.2. Preparation of magnetic Fe_3O_4 nanoparticles

Fe_3O_4 nanoparticles were prepared by the coprecipitation of ferric and ferrous salts in anaerobic conditions at ambient temperature. Fifty milliliters of 1.5 M ammonium hydroxide solution was put into a three-neck, round-bottom flask with magnetic stirrer with N_2 protection. To this, 5 mL of iron solution containing 0.1 M Fe^{2+} and 0.2 M Fe^{3+} in double-distilled water was added slowly by a drop funnel, the color of the suspension turned black immediately, indicating the formation of magnetite. The resulting black precipitate was collected with a strong magnet, and the supernatant was removed from the precipitate by decantation. Deoxygenated double-distilled water was added to wash the powder. The solution was centrifuged for 2 min at a speed of 1800 rpm and the solution was decanted. Centrifugation–redispersion cycles were carried for several times to remove excess ammonia from the remaining solution. Finally, a black precipitate (magnetite) was obtained by freeze-drying.

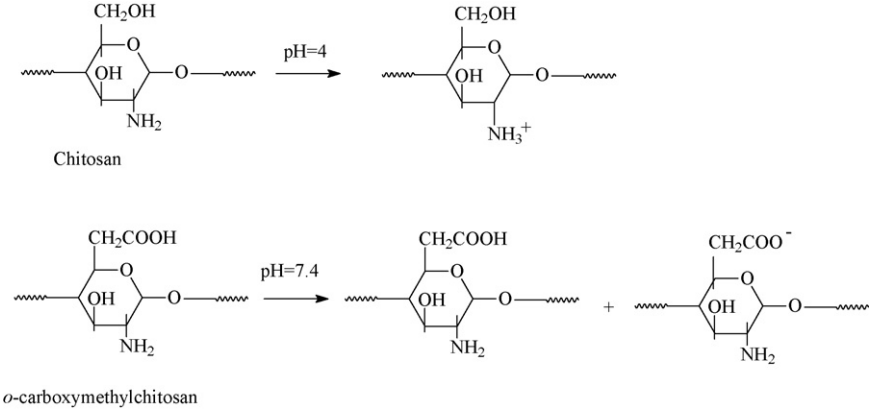

Scheme 1. Charge formation of chitosan and OCMCS in aqueous solution.

2.3. Chitosan and OCMCS surface-modified Fe_3O_4 nanoparticles

For chitosan or OCMCS surface-modified Fe_3O_4 nanoparticles, 10 mg as-prepared black precipitate was dispersed in 10 mL of 0.2 mg/mL of an acidic chitosan solution (pH 4) or 10 mL of 0.2 mg/mL OCMCS neutral aqueous solution (pH 7.4), respectively, and stirred for 12 h at room temperature to ensure the particles were coated evenly. The resulted black dispersions were purified by several centrifugation–redispersion cycles to remove the free CS and OCMCS. The colloidal solution of CS/Fe_3O_4 or OCMCS/Fe_3O_4 magnetic nanoparticles was centrifuged for 10 min at a speed of 25,000 rpm. Finally, CS/Fe_3O_4 and OCMCS/Fe_3O_4 magnetic nanoparticles were obtained by freeze-drying.

2.4. Characterization

The crystal structure of the samples was examined by X-ray diffraction (XRD) with a XD-3A powder diffractometer, using a monochromatized X-ray beam with nickel-filtered Cu Kα radiation in the range of 5–40° (2θ) at 40 kV and 30 mA. The size and morphology of the magnetite nanoparticles were measured by a TE CHAI-12 (Philips) transmission electron microscopy (TEM). The particle size distribution was investigated by using a modified commercial LLS spectrometer (ALV/SP-125, Germany), which was equipped with a solid-state laser (Coherent DPSS) having an output power of 400 mW at λ_0 532.0 nm and an ALV-5000 multi-τ digital time correlator, to perform the dynamic light scattering experiments. Fourier transform infrared (FTIR) spectroscopy was applied to characterize the changes in the chemical structure of Fe_3O_4 nanoparticles after surface stabilization. The magnetization and hysteresis loop were measured at the room temperature with a Lake Shore Model 7300 VSM. The zeta potential of the magnetite suspension was found using a zeta-potential analyzer (Zetaplus, Brookhaven Instruments, USA).

3. Results and discussion

3.1. Stability, particle size and its distribution of colloidal solution

Both CS and OCMCS are supposed to be good surface-active agents for stabilizing aqueous suspension of Fe_3O_4 magnetic nanoparticles because of their polyelectrolyte property. The colloidal stability of resulting magnetic nanoparticles is shown in Fig. 1, which clearly demonstrates that a CS or OCMCS stabilized magnetic nanoparticles exhibits a well-dispersed appearance, while the unmodified dispersion of magnetic nanoparticles precipitates completely.

The particle size and its distribution of the suspension of unmodified, CS and OCMCS stabilized magnetic nanoparticles are shown in Fig. 2. The mean particle radius was measured by DLS is 42 nm with a polydispersity index of 0.262 for CS/Fe_3O_4 nanoparticles, and 38 nm with a polydispersity index of 0.285 for OCMCS/Fe_3O_4 nanoparticles. Though the high polydispersity index suggests that there is still some aggregation of CS and OCMCS stabilized Fe_3O_4 nanoparticles in their suspension, the size of the hydrodynamic radium of CS/Fe_3O_4 or OCMCS/Fe_3O_4 particles is within the nanoscale range. However, the mean particle radius for unmodified magnetic nanoparticles shows 748 nm, suggesting a very fast and strong flocculation.

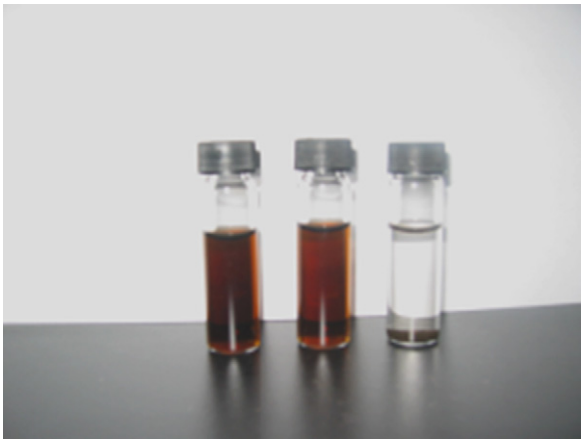

Fig. 1. Stability comparison of colloidal suspension of CS, OCMCS and unmodified magnetic nanoparticles (from left to right) (all the suspensions were centrifuged at 10,000 rpm for 10 min).

Colloidal processing of magnetic nanoparticles has been extensively studied with emphasis on the characteristics of the dispersion as a ferrofluid. Suspensions of magnetic nanoparticles contain van der Waals' forces and magnetic dipole–dipole interactions generated from residual magnetic moments, which tend to agglomerate and flocculate the particles. Ferrofluids composed of magnetic nanoparticles are not only affected by an inhomogeneous particle size distribution, but also by the surface charge of the particles in the solution. A practical method used to stabilize ferrofluids is through electrostatic repulsion, achieved by similar surface charge, which results from the formation of an electrical double layer around the particles. A

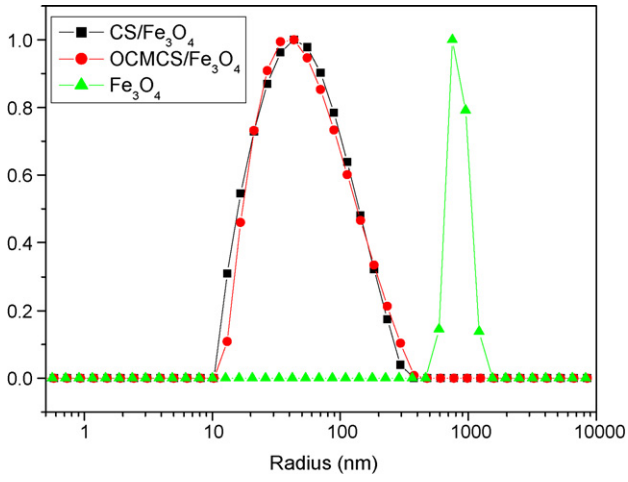

Fig. 2. The hydrodynamic radium and its distribution of colloidal suspension of resulting magnetic nanoparticles determined from DLS at a scattering angle of 90°.

colloidal solution is a suspension in which the dispersed phase is so small that gravitational forces are negligible and particle interactions are dominated by short-range forces, such as van der Waals' attraction and surface charges. The inertia of the dispersed phase is small enough that it exhibits Brownian motion, a random walk driven by momentum transferred through collisions with molecules of the suspending medium (Khalafalla and Reimers, 1973). As above, the magnetic nanoparticles are usually required to graft with nonmagnetic substances to form a stable ferrofluid. Many kinds of natural (e.g., proteins and polysaccharides), synthetic (e.g., polyelectrolytes), and non-ionic polymers (e.g., poly(vinyl alcohol)) have been used for particle coating. The present results expressed that both chitosan and OCMCS are effective to disperse the magnetic Fe_3O_4 nanoparticles. Moreover, the suspension of CS/Fe_3O_4 and OCMCS/Fe_3O_4 nanoparticles can maintain their initial properties more than 6 months, which is very important for its biomedical applications.

3.2. FTIR

The FTIR spectra of unmodified, CS and OCMCS surface-modified magnetic nanoparticles are shown in Fig. 3. Fig. 3(a) shows the peak of 569 cm^{-1}, which is typical characteristic of Fe–O–Fe in Fe_3O_4. However, from Fig. 3(b) and (c), it can be seen that the characteristic peak of Fe–O–Fe shifts to 575 and 583 cm^{-1}, respectively. In addition, the peaks of 1580 and 1425 cm^{-1} appeared in Fig. 3(b) are characteristic absorption bands of chitosan, and the peaks of 1558 and 1406 cm^{-1} bands presented in Fig. 3(c) are characteristic absorption bands of OCMCS. These results proved that CS and OCMCS have been adsorbed onto Fe_3O_4 nanoparticles.

3.3. TEM morphology

TEM was applied to determine the morphology of the magnetite and the results are shown in Fig. 4. It can be seen from Fig. 4 that the resulting magnetic Fe_3O_4 nanoparticles are almost spherical or ellipsoidal. The mean particle size is 14.1 nm with a standard deviation of about 3.5 nm. The average particle size and standard deviation are 16.7 and 3.2 for CS/Fe_3O_4 nanoparticles, respectively. The average particle size and standard deviation are 19.4 and 4.6 nm for OCMCS/Fe_3O_4 nanoparticles, respectively. Though it is difficult to directly observe the adlayer of CS or OCMCS on the Fe_3O_4 nanoparticles from TEM micro-

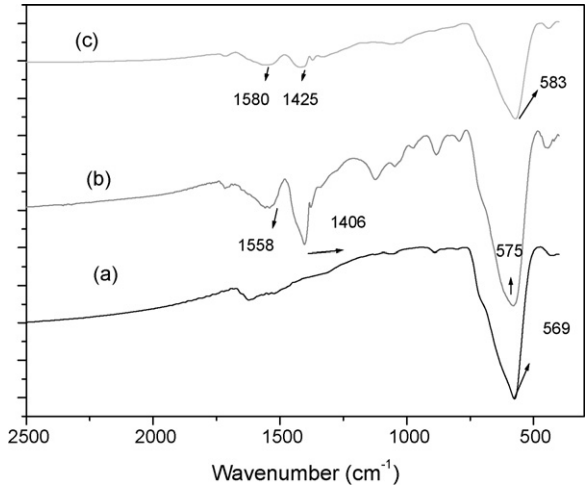

Fig. 3. FTIR spectra of unmodified, CS and OCMCS magnetic nanoparticles.

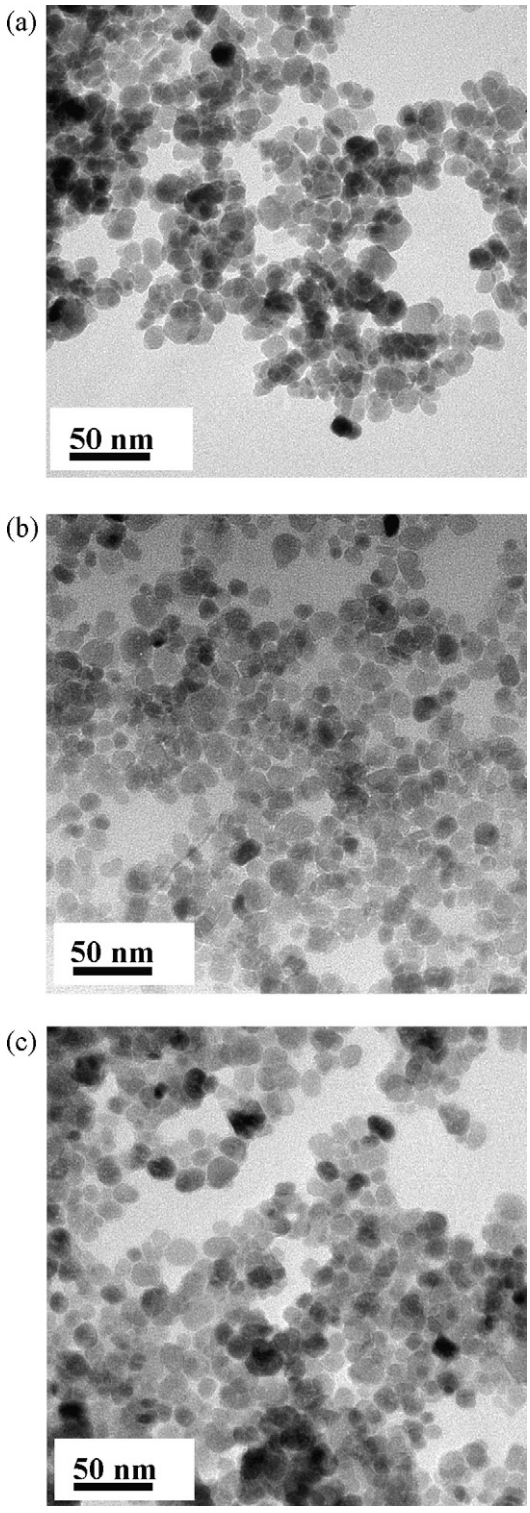

Fig. 4. TEM morphology of (a) unmodified Fe_3O_4 magnetic nanoparticles; (b) CS/Fe_3O_4 magnetic nanoparticles; (c) OCMCS/Fe_3O_4 magnetic nanoparticles.

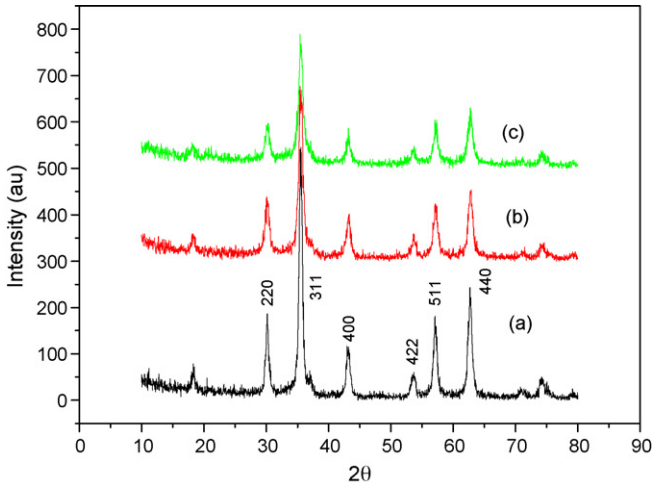

Fig. 5. X-ray powder diffraction patterns of the Fe_3O_4 magnetic nanoparticles.

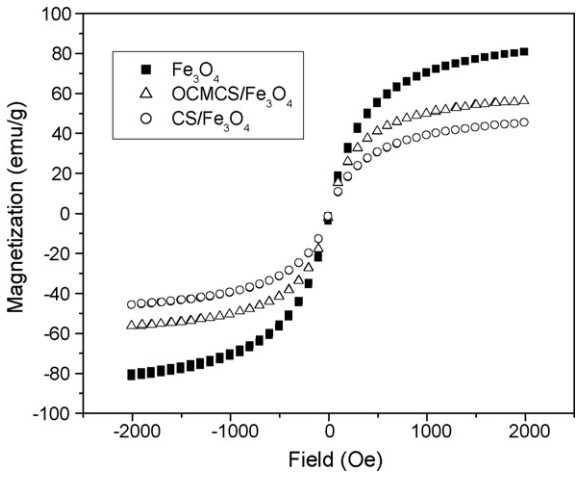

Fig. 6. Magnetization curve for the Fe_3O_4 magnetic nanoparticles at room temperature.

graphs, the dispersing behavior of surface stabilized Fe_3O_4 nanoparticles (Fig. 1(b) and (c)) has obviously been improved in comparison with that of unmodified magnetic nanoparticles (Fig. 1(a)), which exhibits aggregated morphology.

3.4. XRD

To confirm the presence of crystalline Fe_3O_4, CS/Fe_3O_4 and OCMCS/Fe_3O_4 nanoparticles, the structure of the magnetic particles was characterized by XRD and the diffractogram is shown in Fig. 5. There are six diffraction peaks: (2 2 0), (3 1 1), (4 0 0), (4 2 2), (5 1 1) and (4 4 0) in the unmodified Fe_3O_4 particles, which is the standard pattern for crystalline magnetite with spinel structure (Ma et al., 2005). It is clearly seen there is little influence of the dispersant on the structure of magnetic particles, except that the amorphous phase of CS or OCMCS appears as a scattered maximum on the background as seen from Fig. 5(b) and (c).

3.5. Magnetic results

The magnetization of ferromagnetic Fe_3O_4 bulk material is very sensitive to the microstructure of the sample. Superparamagnetism occurs when the particle is small enough that thermal fluctuations (these are of order kT) can overcome the magnetic anisotropy (this is of the order of KV, where K is the anisotropy constant and V is the particle volume). Once this happens the magnetization of the particle is no longer fixed along a certain direction (determined by the easy magnetic direction of the lattice) but appears to be random, in which each particle acts as a big "spin" with suppressed exchange interaction between the particles. The lack of hysteresis is one of the criteria requirements for the identification of the product as superparamagnetic.

Magnetization hysteresis loops at 300 K of unmodified, CS and OCMCS surface-modified Fe_3O_4 magnetic nanoparticles are shown in Fig. 6. The specific magnetism σ_s is 59.0 emu/g, remanence σ_r is 3.6 emu/g, and the coercivity H_c is 28.7 Oe for the uncoated Fe_3O_4 magnetic nanoparticles, while σ_s is 39.1 emu/g, σ_r is 0.5 emu/g and H_c is 4.5 Oe for CS/Fe_3O_4 magnetic nanoparticles, respectively; σ_s is 51.4 emu/g, σ_r is 0.5 emu/g and H_c is 5.0 Oe for OCMCS/Fe_3O_4 magnetic nanoparticles, respectively. The σ_s of the prepared magnetite is high, and the σ_r and H_c are low. It can be seen from Fig. 6 thatσ_s, σ_r, and H_c decrease after the particles are coated. The decrease of the magnetization is attributed to the coating polymer on the magnetic nanoparticles. In our experiment the resulted magnetic nanoparticles were immobilized on the wall of a test tube for 10 s by applying a magnetic field. The saturation magnetization of CS and OCMCS surface-modified Fe_3O_4 magnetic nanoparticles was also found to be enough for magnetic separation as a conventional magnet. This method is advantageous over the other methods to get the polymer-modified magnetites, in which, the saturation magnetization was only found to be 16.3 emu/g caused by the low Fe_3O_4 content (24.3%) in the modified Fe_3O_4 nanoparticles (Ma et al., 2005). And the other magnetic microspheres obtained from copolymerization also contain only small loading of magnetic materials and the process is tedious (Furusawa et al., 1994; Sauzedde et al., 1999).

3.6. Stabilization mechanism

A crucial physical property of colloidal dispersions is the tendency of the particle aggregation. Encounters between particles dispersed in liquid media occur frequently, and the stability of the dispersion is determined by the interaction between the particles during this encounter.

To promote a stable dispersion, short-range repulsive forces are required in order to keep each particle discrete and prevent it from amassing as larger and faster settling agglomerates. Steric hindrance is one of the major surface forces playing an important role in stabilizing suspensions. This is accomplished by the coordination of sterically demanding molecules or polymers that act as protective shields on the oxide surface (Bonnemann et al., 2001). The electronic repulsive force results from creation of an electric double layer around the particles, which provides another mechanism to prevent particle agglomeration.

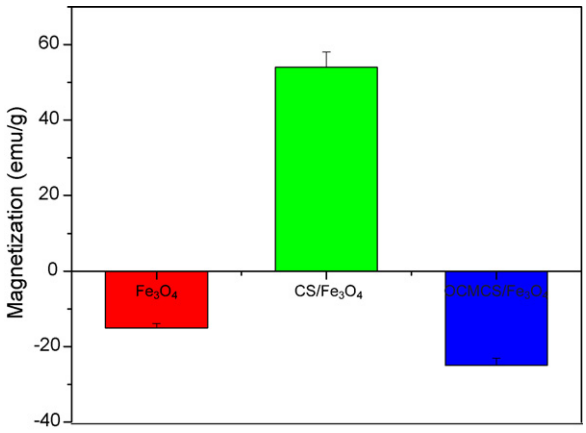

Fig. 7. Zeta potential of colloidal suspension of magnetic nanoparticles (CS/Fe_3O_4 in pH 4, $OCMCS/Fe_3O_4$ in pH 7.4 and Fe_3O_4 in DI water).

In the present system, the stability of suspension originates from tight binding of chitosan or OCMCS on the surface and charge of the particle, which causes repulsion between the particles. It is well known that because of strong intermolecular hydrogen bonding, chitosan and its derivatives are very susceptible for agglomeration by overcoming the barrier from salvation and electrostatic repulsion. Therefore, a zeta-potential measurement is considered as a key parameter for providing an insight into the charge of the resulting Fe_3O_4 nanoparticles. The zeta-potential results are shown in Fig. 7. The zeta potential of suspension for unmodified Fe_3O_4 nanoparticles, CS/Fe_3O_4 nanoparticles and $OCMCS/Fe_3O_4$ nanoparticles is −13.40, +54.20 and −33.45 mV, respectively. The unmodified Fe_3O_4 magnetic nanoparticles precipitate from their aqueous suspension, which suggests that the zeta potential of −13.40 mV for unmodified Fe_3O_4 nanoparticles is not enough to achieve a stable suspension. In pH 4 aqueous CS/Fe_3O_4 system, the amino groups protonate into cationic charges (NH_4^+) (Scheme 1). Therefore, CS can adsorb onto Fe_3O_4 nanoparticles easily by electrostatic attraction, and the amino groups generate positive charge (+54.20 mV) on the Fe_3O_4 nanoparticles surface. As a result, the intermolecular hydrogen bonding of chitosan is suppressed greatly and the stabilization mechanism for the suspension of CS/Fe_3O_4 nanoparticles should be electrostatic repulsion. In addition, CS/Fe_3O_4 nanoparticles with net positive charge can be used to bind with recombinant DNA plasmids to form complex magnetic nanoparticles for targeting genes delivering into cells (Senel et al., 2000; Fang et al., 2001). Also the co-administration of chitosan with drugs and superparamagnetic nanoparticles could enhance the transcellular and paracellular transport of drugs across mucosal epithelium (Chan et al., 2001).

OCMCS has a backbone structure similar to CS, but its *o*-hydroxyl group of each monomer is substituted by a carboxymethyl group through ether bond formation. In pH 7.4 neutral $OCMCS/Fe_3O_4$ system, part of carboxylic acid groups will associate into negative charges and the other carboxyl groups keep molecular form (Scheme 1). According to the literature, an aqueous solution of the uncharged poly(vinyl alcohol) has a strong adhesion to a hydrophilic substance. PVA is known to adsorb on oxide surfaces due to the interaction of hydrogen bonding between the polar groups of the polymer and the surface of the oxide (Lee and Somasundaran, 1989). In our case, OCMCS with functional carboxyl groups is supposed to be chemisorbed on the surface of Fe_3O_4 by the coordination of "Fe" of Fe_3O_4 and "O" of carboxyl groups in OCMCS molecules (concluded according to FTIR results). The partly charged carboxyl groups make Fe_3O_4 magnetic nanoparticles negative (−33.45 mV). Accordingly, the intermolecular hydrogen bonding of OCMCS decreases greatly and the stabilization mechanism for the suspension of $OCMCS/Fe_3O_4$ nanoparticles is also the electrostatic repulsion. In addition, using the carboxylic moiety as a binding site, various molecules (e.g., DNA, proteins), and antibodies, could be immobilized on the $OCMCS/Fe_3O_4$ nanoparticles for potential specific applications, such as the magnetically targeted drug carriers. Moreover, $OCMCS/Fe_3O_4$ nanoparticles are supposed to provide a better association with a hydrophobic drug due to the amphiphilic property of OCMCS. A hydrophobic drug should be located between the OCMCS layer and Fe_3O_4 nanocore. The research on the targeted release of anticancer drugs from these complex superparamagnetic nanoparticles has been investigated in our lab. Magnetic nanoparticles are generally surface modified with hydrophilic polymers such as albumin (Renshaw et al., 1986), dextran (Molday and Mackenzie, 1982), and starch (Veiga et al., 2000) to disperse them in an aqueous vehicle; however, nanoparticles stabilized in this way have limited applications for drug delivery primarily because of the difficulty of loading these formulations with high doses of therapeutic agents, and especially with water-insoluble drugs. High drug loading on a drug carrier system is necessary to achieve a therapeutic dose of the drug in the target tissue/organ effectively. Rapid dissociation of drug from nanoparticles may induce its premature release in the blood stream, and hence the efficacy of the carrier system to target the drug to the desired tissue/organ and retain it there for a sustained period of time could be significantly reduced. The present procedure is simple and effective process for the preparation of well-dispersed aqueous suspension of magnetite nanoparticles in comparison with the previous protocols reported in the literature.

4. Conclusions

The biocompatible chitosan and OCMCS have been proved be an effective dispersant to prepare the well-dispersed suspension of magnetic Fe_3O_4 nanoparticles. The Fe_3O_4 nanoparticles were fully characterized with regard to their morphology, magnetic properties, composition and size distribution by TEM, VSM, FTIR and DLS. The adsorption mechanisms of CS and OCMCS onto magnetic Fe_3O_4 nanoparticles are electrostatic attraction and coordination interaction, respectively. The stabilization mechanism of CS and OCMCS are believed to be electrostatic repulsive. The stable suspension of CS/Fe_3O_4 magnetic nanoparticles has net positive charge and OCMCS stabilized magnetic Fe_3O_4 nanoparticles have functional carboxyl groups.

Acknowledgements

This research was supported by a Natural & Scientific grant of Jiangsu Province, Project BK2006072 and No. 05KJB430149 (China).

References

Abu-Much, R., Merifor, U., Frydman, A., Gedanken, A., 2006. Formation of a three-dimensional microstructure of Fe_3O_4–poly(vinyl alcohol) composite by evaporating the hydrosol under a magnetic field. J. Phys. Chem. B 110, 8194–8203.

Artursson, P., Lindmark, T., Davis, S.S., Illum, L., 1994. Effect of chitosan of chitosan on the permeability of monolayers of intestinal epithelial-cells (Caco-2). Pharm. Res. 11, 1358–1361.

Bonnemann, H., Richards, R.M., 2001. Nanoscopic metal particles—synthetic methods and potential applications. Eur. J. Inorg. Chem. 10, 2455–2480.

Chan, D.C.F., Kirpotin, D.B., Bunn, P.A., 1993. Synthesis and evaluation of colloidal magnetic iron-oxides for the site-specific radiofrequency-induced hyperthermia of cancer. J. Magn. Magn. Mater. 122, 374–378.

Chan, V., Mao, H.Q., Leong, K.W., 2001. Chitosan-induced perturbation of dipalmitoyl-*sn*-glycero-3-phosphocholine membrane bilayer. Langmuir 17, 3749–3756.

Chang, Y.C., Chang, S.W., Chen, D.H., 2006. Magnetic chitosan nanoparticles: studies on chitosan binding and adsorption of Co(II) ions. React. Funct. Polym. 66, 335–341.

Chouly, C., Pouliquen, D., Lucet, I., Jeune, J.J., Jallet, P., 1996. Development of superparamagnetic nanoparticles for MRI: effect of particle size, charge and surface nature on biodistribution. J. Microencapsul. 13, 245–255.

Dyal, A., Loos, K., Noto, M., Chang, S.W., Spagnoli, C., Shafi, K.V.P.M., Ulman, A., Cowman, M., Gross, R.A., 2003. Activity of *Candida rugosa* lipase immobilized on gamma-Fe_2O_3 magnetic nanoparticles. J. Am. Chem. Soc. 125, 1684–1685.

Fang, N., Chan, V., 2003. Chitosan-induced restructuration of a mica-supported phospholipid bilayer: an atomic force microscopy study. Biomacromolecules 4, 1596–1604.

Fang, N., Chan, V., Wan, K.T., Mao, H.Q., Leong, K.W., 2001. Interactions of phospholipid bilayer with chitosan: effect of molecular weight and pH. Biomacromolecules 2, 1161–1168.

Fried, T., Shemer, G., Markovich, G., 2001. Ordered two-dimensional arrays of ferrite nanoparticles. Adv. Mater. 13, 1158.

Furusawa, K., Nagashima, K., Anzai, C., 1994. Synthetic process to control the total size and component distribution of multilayer magnetic composite-particles. Colloid Polym. Sci. 272, 1104–1110.

Gas, J., Poddar, P., Almand, J., Srinath, S., Srikanth, H., 2006. Superparamagnetic polymer nanocomposites with uniform Fe_3O_4 nanoparticle dispersions. Adv. Funct. Mater. 16, 71–75.

Guo, L., Pei, G.L., Wang, T.J., Wang, Z.W., Jin, Y., 2007. Polystyrene coating of Fe_3O_4 particles using dispersion polymerization. Colloids Surf. A: Physicochem. Eng. Aspects 293, 58–62.

Harris, L.A., Goff, J.D., Carmichael, A.Y., Riffle, J.S., Harburn, J.J., Saunders, M., 2003. Magnetite nanoparticle dispersions stabilized with triblock copolymers. Chem. Mater. 15, 1367–1377.

Jordan, A., Scholz, R., Wust, P., Schirra, H., Schiestel, T., Schmidt, H., Felix, R., 1999. Endocytosis of dextran and silan-coated magnetite nanoparticles and the effect of intracellular hyperthermia on human mammary carcinoma cells in vitro. J. Magn. Magn. Mater. 194, 185–196.

Khalafalla, S.E., Reimers, G.W., 1973. US Patent 3,764,540.

Kim, D.K., Zhang, Y., Kehr, J., Klason, T., Bjelke, B., Muhammed, M., 2001a. Characterization and MRI study of surfactant-coated superparamagnetic nanoparticles administered into the rat brain. J. Magn. Magn. Mater. 225, 256–261.

Kim, D.K., Zhang, Y., Voit, W., Rao, K.V., Muhanned, M., 2001b. Synthesis and characterization of surfactant-coated superparamagnetic monodispersed iron oxide nanoparticles. J. Magn. Magn. Mater. 225, 30–36.

Kofuji, K., Ito, T., Murata, Y., Kawashima, S., 2001. Biodegradation and drug release of chitosan gel beads in subcutaneous air pouches of mice. Biol. Pharm. Bull. 24, 205–208.

Lee, L., Somasundaran, T.P., 1989. Adsorption of polyacrylamide on oxide minerals. Langmuir 5, 854–860.

Lubbe, A.S., Bergemann, C., Riess, H., 1996. Clinical experiences with magnetic drag targeting: a phase I study with 4′-epidoxorubicin in 14 patients with advanced solid tumors. Cancer Res. 56, 4686–4693.

Ma, Z.Y., Guan, Y.P., Liu, H.Z., 2005. Synthesis and characterization of micron-sized monodisperse superparamagnetic polymer particles with amino groups. J. Polym. Sci. A: Polym. Chem. 43, 3433–3439.

Mahapatra, S., Pramanik, N., Ghosh, S.K., Pramanik, P., 2006. Synthesis and characterization of ultrafine poly(vinylalcohol phosphate) coated magnetite nanoparticles. Nanosci. Nanotechnol. 6, 823–829.

Mann, S., Hannington, J.P., 1988. Formation of iron-oxides in unilamllar vesicles. J. Colloid Interf. Sci. 122, 326–335.

Mao, H.Q., Roy, K., Truong-Le, V.L., Lin, K.Y., Wang, Y., August, J.T., Leong, K.W., 2001. Chitosan–DNA nanoparticles as gene carriers: synthesis, characterization and transfection efficiency. J. Control. Release 70, 399–421.

Molday, R.S., Mackenzie, D., 1982. Immunospecific ferromagnetic iron-dextran reagents for the labeling and magnetic separation of cells. J. Immunol. Methods 52, 353–367.

Morales, M.A., Jain, T.K., Labhasetwar, V., Leslie-Pelecky, D.L., 2005. Magnetic studies of iron oxide nanoparticles coated with oleic acid and pluronic (R) block copolymer. J. Appl. Phys. 97, Art. No. 10Q905 Part 3.

Neuberger, T., Schopf, B., Hofmann, H., Hofmann, M., Rechenberg, B.V., 2005. Superparamagnetic nanoparticles for biomedical applications: possibilities and limitations of a new drug delivery system. J. Magn. Magn. Mater. 293, 483–496.

Renshaw, P.F., Owen, C.S., McLaughlin, A.C., Frey, T.G., Leigh Jr., J.S., 1986. Ferromagnetic contrast agents—a new approach. Magn. Reson. Med. 3, 217–225.

Reynolds, C.H., Annan, N., Beshah, K., Huber, J.H., Shaber, S.H., Lenkinsi, R.E., Wortman, J.A., 2000. Gadolinium-loaded nanoparticles: new contrast agents for magnetic resonance imaging. J. Am. Chem. Soc. 122, 8940–8945.

Roy, K., Mao, H.Q., Huang, S.K., Leong, K.W., 1999. Oral gene delivery with chitosan–DNA nanoparticles generates immunologic protection in a murine model of peanut allergy. Nat. Med. 5, 387–391.

Sauzedde, F., Elaissari, A., Pichot, C., 1999. Hydrophilic magnetic polymer latexes. 2. Encapsulation of adsorbed iron oxide nanoparticles. Colloid Polym. Sci. 277, 1041–1050.

Senel, S., Kremer, M.J., Kas, S., Wertz, P.W., Hincal, A.A., Squier, C.A., 2000. Enhancing effect of chitosan on peptide drug delivery across *Buccal mucosa*. Biomaterials 21, 2067–2071.

Shafi, K.V.P.M., Ulman, A., Yan, X., Yang, N.L., Estourbes, C., White, H., Rafalovich, M., 2001. Sonochemical synthesis of functionalized amorphous iron oxide nanoparticles. Langmuir 17, 5093–5097.

Shen, L.F., Laibinis, P.E., Hatton, T.A., 1999. Bilayer surfactant stabilized magnetic fluids: synthesis and interactions at interfaces. Langmuir 15, 447–453.

Shieh, D.B., Cheng, F.Y., Su, C.H., Yeh, C.S., Wu, M.T., Wu, Y.N., Tsai, C.Y., Wu, C.L., Chen, D.H., Chou, C.H., 2005. Aqueous dispersions of magnetite nanoparticles with NH3+ surfaces for magnetic manipulations of biomolecules and MRI contrast agents. Biomaterials 26, 7183–7191.

Thanou, M., Verhoef, J.C., Junginger, H.E., 2001. Oral drug absorption enhancement by chitosan and its derivatives. Adv. Drug Delivery Rev. 52, 117–126.

Thode, K., Luck, M., Schroder, W., Semmler, W., Blunk, T., Muller, R.H., Kresse, M., 1997. The influence of the sample preparation on plasma protein adsorption patterns on polysaccharide-stabilized iron oxide particles and N-terminal microsequencing of unknown proteins. J. Drug Target 5, 35–43.

Veiga, V., Ryan, D.H., Sourty, E., Llanes, F., Marchessault, R.H., 2000. Formation and characterization of superparamagnetic cross-linked high amylose starch. Carbohydr. Polym. 42, 353–357.

Wan, S., Huang, J.S., Guo, M., Zhang, H.K., Cao, Y.J., Yan, H.S., Liu, K.L., 2007. Biocompatible superparamagnetic iron oxide nanoparticle dispersions stabilized with poly(ethylene glycol)–oligo(aspartic acid) hybrids. J. Biomed. Mater. Res. 80A, 946–954.

Xie, X., Zhang, X., Zhang, H., Chen, D.P., Fei, W.Y., 2004. Preparation and application of surface-coated superparamagnetic nanobeads in the isolation of genomic DNA. J. Magn. Magn. Mater. 277, 16–23.

Zhang, Y., Kohler, N., Zhang, M., 2002. Surface modification of superparamagnetic magnetite nanoparticles and their intracellular uptake. Biomaterials 23, 1553–1561.

Zhi, J., Wang, Y.J., Lu, Y.C., Ma, J.Y., Luo, G.S., 2006. In situ preparation of magnetic chitosan/Fe_3O_4 composite nanoparticles in tiny pools of water-in-oil microemulsion. React. Funct. Polym. 66, 1552–1558.

Zhu, A.P., Chan, M.B., Dai, S., Li, L., 2005a. The aggregation behavior of *o*-carboxymethylchitosan in dilute aqueous solution. Colliod Surf. B: Biointerf. 43, 143–149.

Zhu, A.P., Fang, N., Chan-Park, M.B., Chan, V., 2005b. Interaction between *o*-carboxymethylchitosan and dipalmitoyl-*sn*-glycero-3-phosphocholine bilayer. Biomaterials 26, 6873–6879.

Zhu, A.P., Liu, J.H., Ye, W.H., 2006. Effective loading and controlled release of camptothecin by *o*-carboxymethylchitosan aggregates. Carbohydr. Polym. 63, 89–96.